ELSEVIER

Palaeogeography, Palaeoclimatology, Palaeoecology 111 (1994) 249–262

PALAEO GEOGRAPHY CLIMATOLOGY ECOLOGY

Magnetostratigraphy and biostratigraphy of an Anisian–Ladinian (Middle Triassic) boundary section from Hydra (Greece)

Giovanni Muttoni [a], James E.T. Channell [b], Alda Nicora [a], Roberto Rettori [c]

[a] *Dipartimento di Scienze della Terra, Università degli Studi di Milano, via Mangiagalli 34, 20133 Milano, Italy*
[b] *Department of Geology, University of Florida, 1112 Turlington Hall, Gainesville, FL 32611, USA*
[c] *Dipartimento di Scienze della Terra, Università degli Studi di Perugia, Piazza Università, 06100 Perugia, Italy*

Received 24 September 1993; revised and accepted 21 February 1994

Abstract

On the island of Hydra, the Anisian/Ladinian boundary is exposed in a 24 m thick section of nodular reddish Han-Bulog Limestone. This paper is focused on the magnetostratigraphy and conodont biostratigraphy of this section. The Anisian/Ladinian boundary is defined by the First Appearance Datum (FAD) of the conodont species *Gondolella trammeri* Kozur (base of the Nevadites ammonoid zone), and occurs in a normal polarity zone. Microfacies analysis has distinguished a lower and upper lithofacies recording gradual shallowing from pelagic conditions to a platform margin paleoenvironment.

1. Introduction

The island of Hydra (Fig. 1) is part of the Subpelagonian Zone and exhibits a well preserved Permian to Jurassic sedimentary sequence (Römermann et al., 1981; Baud et al., 1991; Angiolini et al., 1992). Angiolini et al. (1992) reported a section with Late Illyrian (Late Anisian) conodonts outcropping near the monastery of Aghia Triada (Fig. 1). The section is comprised of the Han-Bulog Limestone, a red nodular facies widespread in the Tethyan Triassic. Angiolini et al. (1992) inferred the location of the Anisian–Ladinian boundary in this section on the basis of lithological correlations to other sections outcropping on the island.

This paper documents the magnetostratigraphy of the Aghia Triada section and verifies the presence of the Anisian–Ladinian boundary by detailed conodont biostratigraphy. A short section at Aghia Marina (Fig. 1), which is the same age as part of the Aghia Triada section has also been studied.

2. Geological setting

The Permian to Jurassic sedimentary sequence of Hydra is arranged in four major thrust sheets, dislocated by transcurrent faults (Angiolini et al., 1992) (Fig. 1). The beds generally dip northward, such that the Permian crops out along the southern side of the island and the Triassic–Jurassic along the northern side (for a detailed geological map, see Angiolini et al., 1992). The Triassic succession comprises a few meters of Scythian quartzarenites (Aghios Nikolaos Fm.) overlain by the transition to a thick carbonate platform (Eros Lst.). The platform drowned during the Pelsonian–Illyrian (Late Anisian) (Fig. 2), and was overlain by a pelagic sequence comprising a few tens of meters of ammonoid and conodont-bearing red nodular limestones with associated acid tuffs (Han-Bulog Lst., Late Pelsonian–Early Ladinian). Above the Han-Bulog Lst., the Ladinian to Upper Triassic sequence of the eastern part of the island (Ormos

SSDI 0031-0182(94)00019-5

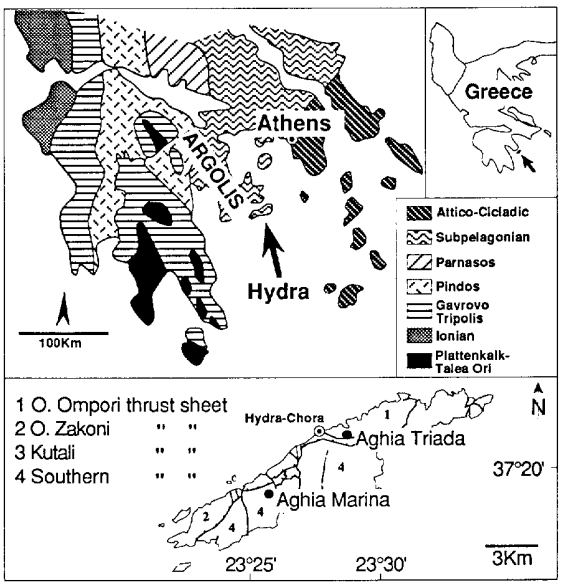

Fig. 1. Geological sketch map of the Peloponnesus (after Mountrakis et al., 1987) showing the location of Hydra island. The major tectonic features of the island (after Angiolini et al., 1992) and section locations are indicated.

Ompori thrust sheet) is represented by a new carbonate platform (Pantokrator Lst.). In the southern thrust sheet, however, the Han-Bulog Lst. is overlain by 60–200 m of thin-bedded cherty limestones (Adhami Lst.) indicating continued pelagic conditions (Figs. 1 and 2). The Jurassic Ammonitico Rosso and Radiolarite sequence marks the drowning of the Pantokrator Platform and development of uniform pelagic conditions.

The island of Hydra is structurally part of the Argolis peninsula, which lies a few kilometers to the NW (Fig. 1). The Argolis peninsula is affected by Late Jurassic (eohellenic) and Late Eocene/Early Oligocene nappe emplacement (Baumgartner, 1985). On Hydra it is not possible to separate the contribution of the Late Jurassic and Tertiary deformation phases (Jacobshagen, pers. comm., 1993).

This paper is focused on the Late Pelsonian–Early Ladinian Han-Bulog Limestone. This formation was labeled "Hallstatt facies" by Renz (1906) and Römermann et al. (1981), and Bulog Lst. by Renz (1931). Angiolini et al. (1992) preferred the name Han-Bulog Lst., due to its closer similarity with the Han-Bulog Lst. of the Dinarides than with the Hallstatt Lst. of the Northern Calcareous Alps. The Han-Bulog Lst. of Hydra consists of cm to dm-thick beds of grey and red nodular limestones, locally rich in ammonoids. The thickness of the Han-Bulog Lst. varies from 0 to 50 m. In the southern thrust sheet, the thickness is discontinuous and reaches a maximum of 7 m. On the other hand, in the Ormos Ompori and Ormos Tsakoni thrust sheets, higher subsidence resulted in a greater thickness and lateral continuity of the formation (Wendt, 1973; Angiolini et al., 1992). The Aghia Triada section, entirely comprised of the Han-Bulog Lst. (24.6 m thick), is located in the Ormos Ompori thrust sheet, near the Aghia Triada monastery, east of the village of Hydra-Chora (Fig. 1). It has been studied for its Illiryan conodonts (section H in Angiolini et al., 1992), as well as for Illyrian ammonoids (Renz, 1931). The Aghia Marina section is located in the Southern thrust sheet, near the Aghia Marina chapel (Fig. 1). It is more condensed than the Aghia Triada section, and it is composed of a few meters of Han-Bulog Lst. It corresponds to the lowermost part of section A of Angiolini et al. (1992).

3. Lithostratigraphy

The Aghia Triada section is 24.6 m thick and is lithologically fairly homogeneous (Fig. 3).

(1) From 0.0 to 7.2 m: centimeter-thick beds of grey to pink-grey nodular limestones alternating with red marls and nodules bounded by red matrix, rich in ammonoids, crinoids and filaments (pelagic bivalves). Calcarenites and calcareous breccia levels made up of grey to pink millimetric to centimetric limestone clasts in a red matrix with filaments are also present.

(2) From 7.2 to 9.0 m: centimetre-thick planar beds of red limestones.

(3) From 9.0 to 15.0 m: centimetre-thick beds of filament-bearing grey to pink-grey limestone nodules with red marly matrix.

(4) From 16.0 to 24.6 m: grey limestones with calcarenitic levels. An upward disappearance of filaments is observed.

Microfacies analysis distinguishes two basic

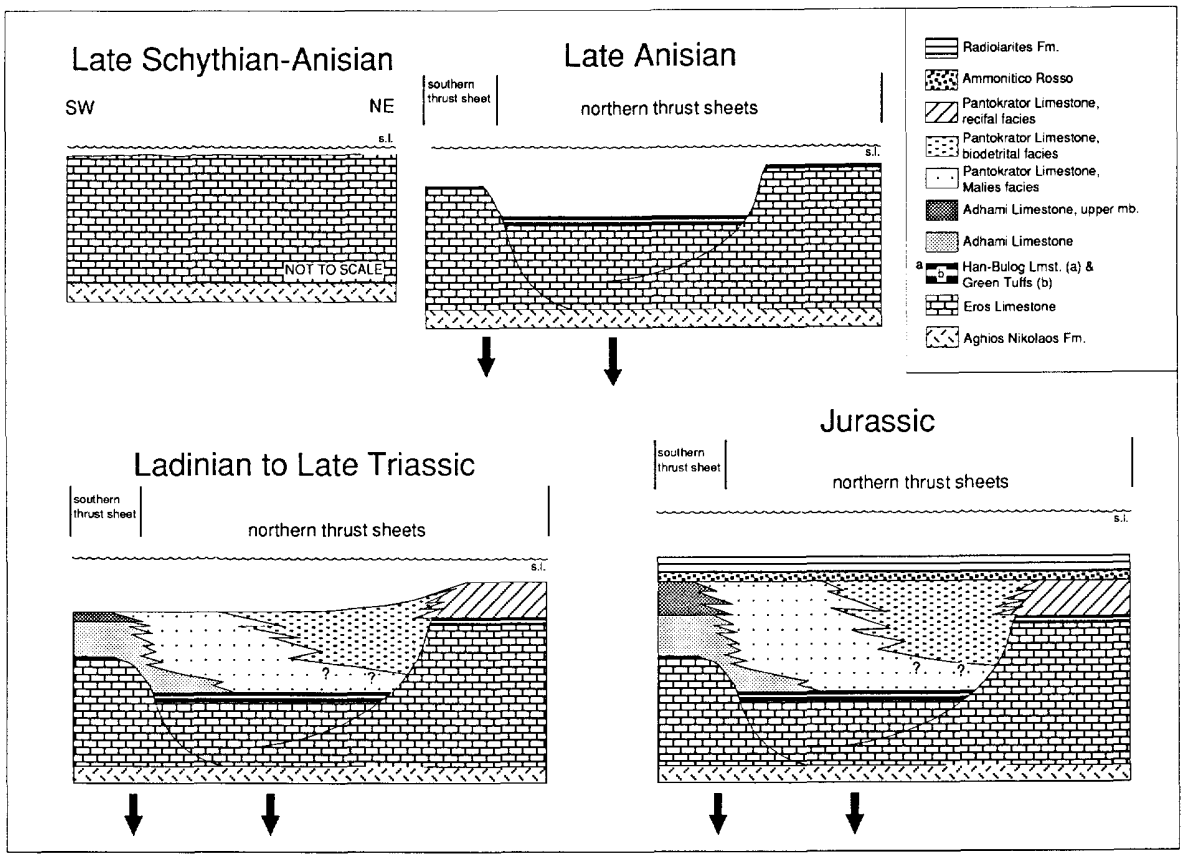

Fig. 2. Paleogeographic reconstruction of the Late Scythian to Jurassic sedimentation on Hydra. See text for discussion.

lithofacies, a lower and an upper lithofacies. They show transitional features reflecting the evolution from pelagic conditions (Han Bulog Lst.) to a carbonate platform (Pantokrator) (see also Römermann, 1981; Schäffer and Senowbari-Daryan, 1984; Angiolini et al., 1992; Rettori et al., 1994).

In the lower lithofacies (toe-of-slope and basin facies) (base to 16.0 m), floatstones of intraformational soft clasts and "hard" clasts are enclosed in a micritic reddish matrix. The "soft" clasts consist of detritic bioclastic wackestones and packstones, and the "hard" clasts of algal and encrusting organism-bearing boundstones. The biota present in the algal boundstones and in the packstones are extremely diversified: gastropods, bivalves, echinoderms, tufts of blue-green algae, green algae [*Cayeuxia* sp., *Ortonella* sp., *Thaumatoporella parvovesiculifera* (Rainieri), bioclasts of dasyclads such as *Gyroporella* sp.], Porostromata and Spongiostromata sensu Pia, problematica [*Tubiphytes obscurus* Maslov, *T. carinthiacus* (Flügel), ?*T. gracilis* Schäfer and Senowbari-Daryan], microproblematica encrusting organisms [*Bacinella irregularis* Radoicic, *B. ordinata* Pantic, *Microtubus communis* Flügel, *Macrotubus babai* Fois (in Fois and Gaetani, 1981), *Koivaella* cfr. *K. permiensis* Chuvashov]. Foraminifers are very rare and exclusively represented by *Earlandia amplimuralis* Pantic, *E. gracilis* Pantic and *Aeolisaccus dunningtoni* Elliot, other than encrusting forms referable to the genus *Nubecularia* sp.

In the upper lithofacies (foreslope to margin facies) (17.0 m to 24.6 m) there is considerably

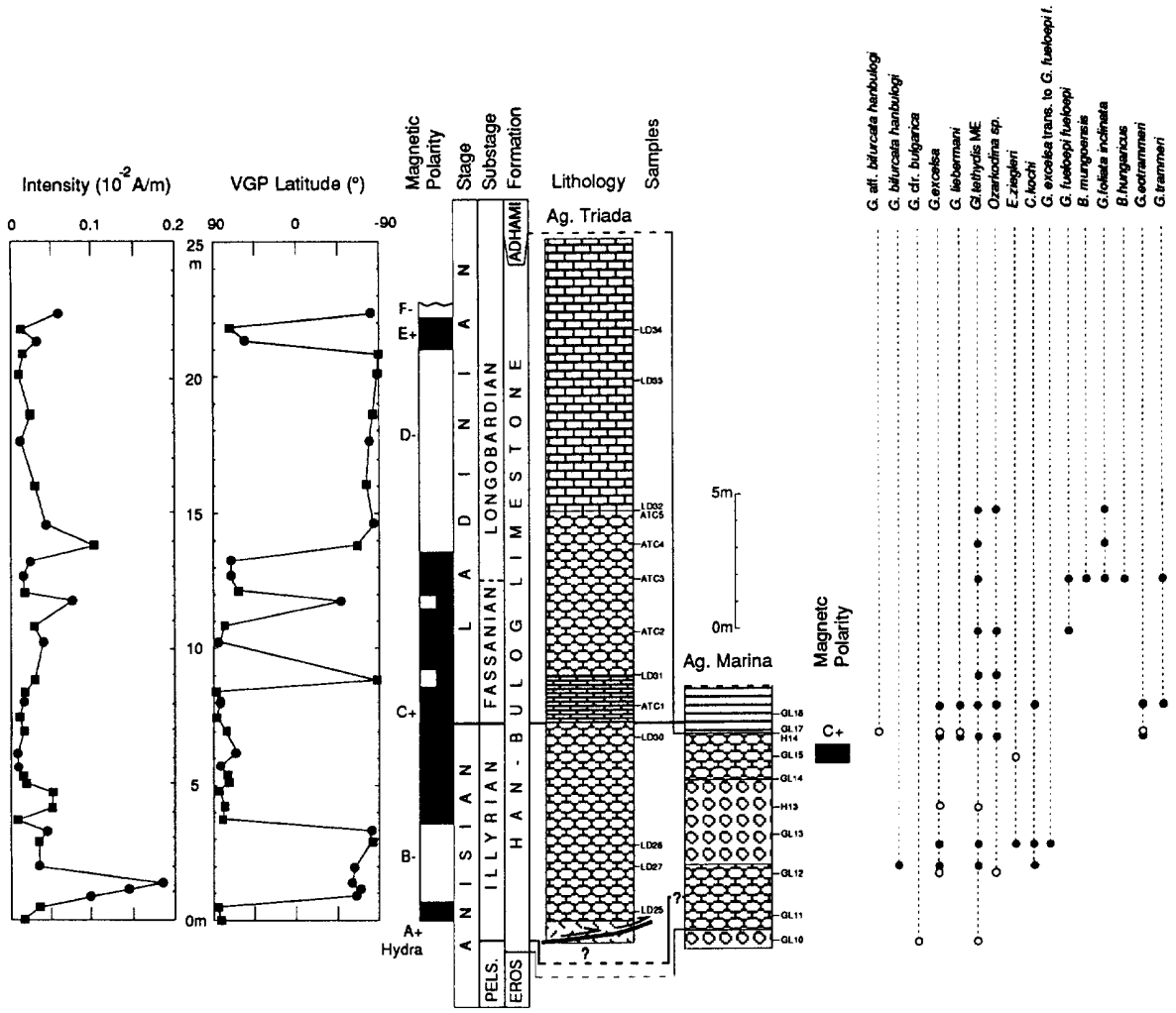

Fig. 3. Aghia Triada and Aghia Marina sections. The VGPs latitudes and the intensity values of the NRM are plotted as function of stratigraphic position. Squares represent the mean of two specimens from the same sample, whereas circles represent one specimen only. Black and white intervals in the block diagram represent normal and reversed polarity, respectively. Half bars indicate uncertain polarity designation based on single samples/specimens. Polarity zones are designated by letters with the prefix *Hydra* in ascending alphabetical order, followed by "+" (normal) or "-" (reversed). The distribution of important conodont species is given and this distribution is the basis for the stage/substage subdivision indicated. Black dots and white dots represent Aghia Triada and Aghia Marina conodons, respectively. The Anisian/Ladinian boundary is positioned 7.3 m above the base of the Aghia Triada section, in the polarity zone Hydra C+.

less matrix, compared to the lower lithofacies and an increasing concentration of grainstones and rudstones of margin-derived sediments. Subordinate packstones are also present. The grainstones and rudstones mainly consist of loose sediment and paleontologically diversified boundstones. The paleontological assemblage is slightly more abundant and diversified than that of the lower lithofacies: foraminifers [*E. amplimuralis* Pantic, *E. gracilis* Pantic, Duostominidae, Lituolidae (*Reophax* sp./*Ammobaculites* sp.), "Trochamminidae", Endotriadidae, ?*Palaeolituo-*

nella meridionalis (Luperto), encrusting foraminifers as *Nubecularia* sp. and *Tolypammina* cfr. *T. gregaria* Wendt], microproblematica (*Baccanella floriformis* Pantic, *Muranella sphaerica* Borza, *Globochaete gregaria* Schäfer and Senowbari-Daryan, *Poripheritubus buseri* Senowbari-Daryan, *B. irregularis, B. ordinata, M. communis, K.* cfr. *K. permiensis, M. babai*). The algal encrusting organisms of the boundstones are dominated by problematica (*T. obscurus, T. carinthiacus, ?T. gracilis*), Porostromata, Spongiostromata and green algae (*Cayeuxia* sp.). Sphinctozoa (*Colospongia catenulata catenulata* Jablonsky, *Solenolmia manon manon* (Munster), *Cryptocoelia* aff. *C. zitteli* Steinmann) are common either in the boundstones or as detritus in the grainstones.

The Aghia Marina section is about 7.5 m thick (Fig. 3) and consists of:

(1) from 0.0 to 2.4 m: centimeter-thick beds of grey to red nodular limestones rich in filaments (pelagic bivalves), directly overlying the Scythian–Anisian carbonate platform of Eros Limestone.

(2) From 2.4 to 5.8 m: decimeter-thick beds of calcareous breccia.

(3) From 5.8 to 7.5 m: centimetre-thick beds of red nodular limestones with the proportion of red matrix increasing up-section. This level has been sampled for paleomagnetic analysis. No detailed microfacies analysis has been performed in the Aghia Marina section.

4. Biostratigraphy

Angiolini et al. (1992) reported the presence of Late Illyrian conodonts (among them *Gondolella excelsa* (Mosher), *G. eotrammeri* Krystyn and *G. liebermani* Kovács and Krystyn, sample LD30, Fig. 3 of this paper) in the lower part of the Aghia Triada section. The same authors dated the Aghia Marina section as Late Pelsonian–Early Ladinian (Fig. 3), on the basis of conodont biostratigraphy and direct lithologic correlations with coeval sections outcropping nearby. In this paper, a more detailed sampling carried out at Aghia Triada has led to the identification of Early and Middle Ladinian conodonts (Fig. 3). The conodont fauna is neither abundant nor well preserved. However, this does not invalidate the biostratigraphy.

The biostratigraphic definition of the Anisian/Ladinian boundary is still in dispute. Three possible positions for the base of the Ladinian using Western Tethys ammonoid zones have been recently discussed (Gaetani, 1993) (Fig. 4): (1) at the base of the Reitzi/Kellnerites Zone; (2) at the base of the Nevadites Zone; (3) at the base of the Curionii Zone. In the conodont stratigraphy, no remarkable events characterize the base of the Reitzi/Kellnerites Zone, where slender, elongated forms with anteriorward shifting of the basal pit occur in the *G. constricta* lineage. These forms are already developed in the late Trinodosus Zone (Kovács et al., 1990) and/or in the *Parakellnerites meriani* B horizon (Kovács, 1994). The base of the Curionii Zone is inconspicuously marked by the appearance of the *Gondolella transita* group, however, near to the First Appearance Datum (FAD) of the genus *Nevadites* at the base of the Nevadites ammonoid zone, the conodont *Gondolella trammeri* Kozur appears. Following Krystyn (1983) and Kovács et al. (1990), the FAD of *G. trammeri* is used in the Aghia Triada section as the marker for the Anisian/Ladinian boundary, which is therefore placed between samples LD30 and ATC1 at 7.30 m (Fig. 3).

G. eotrammeri, G. trammeri, G. liebermani, G. excelsa and *Gladigondolella tethydis* Multi Element (ME) occur in sample ATC1 (Fig. 3). *G. fueloepi fueloepi* Kovács and *Gl. tethydis* ME occur in sample ATC2. *Budurovignathus hungaricus* (Kozur and Vegh), *B. mungoensis* (Diebel), *G. trammeri, G. foliata inclinata* Kovács, *G. fueloepi fueloepi, Gl. tethydis* ME characterize the conodont fauna of sample ATC3. *G. foliata inclinata, Gl. tethydis* ME occur in samples ATC4 and ATC5 (Fig. 3).

According to the conodont distributions of Krystyn (1983) and Kovács (1994) (Fig. 4D), *G. liebermani* occurs from the upper Trinodosus Zone (Late Illyrian) to the top of the *Hyparpadites liepoldti* horizon (middle Reitzi/Kellnerites Zone, Kovács, 1994) (Fig. 4). *G. eotrammeri* ranges from the lower part of the Reitzi/Kellnerites Zone to the lower part of the Nevadites Zone. *G. trammeri* occurs from the base of the Nevadites to the base of the Regoledanus Zones. *G. fueloepi fueloepi*

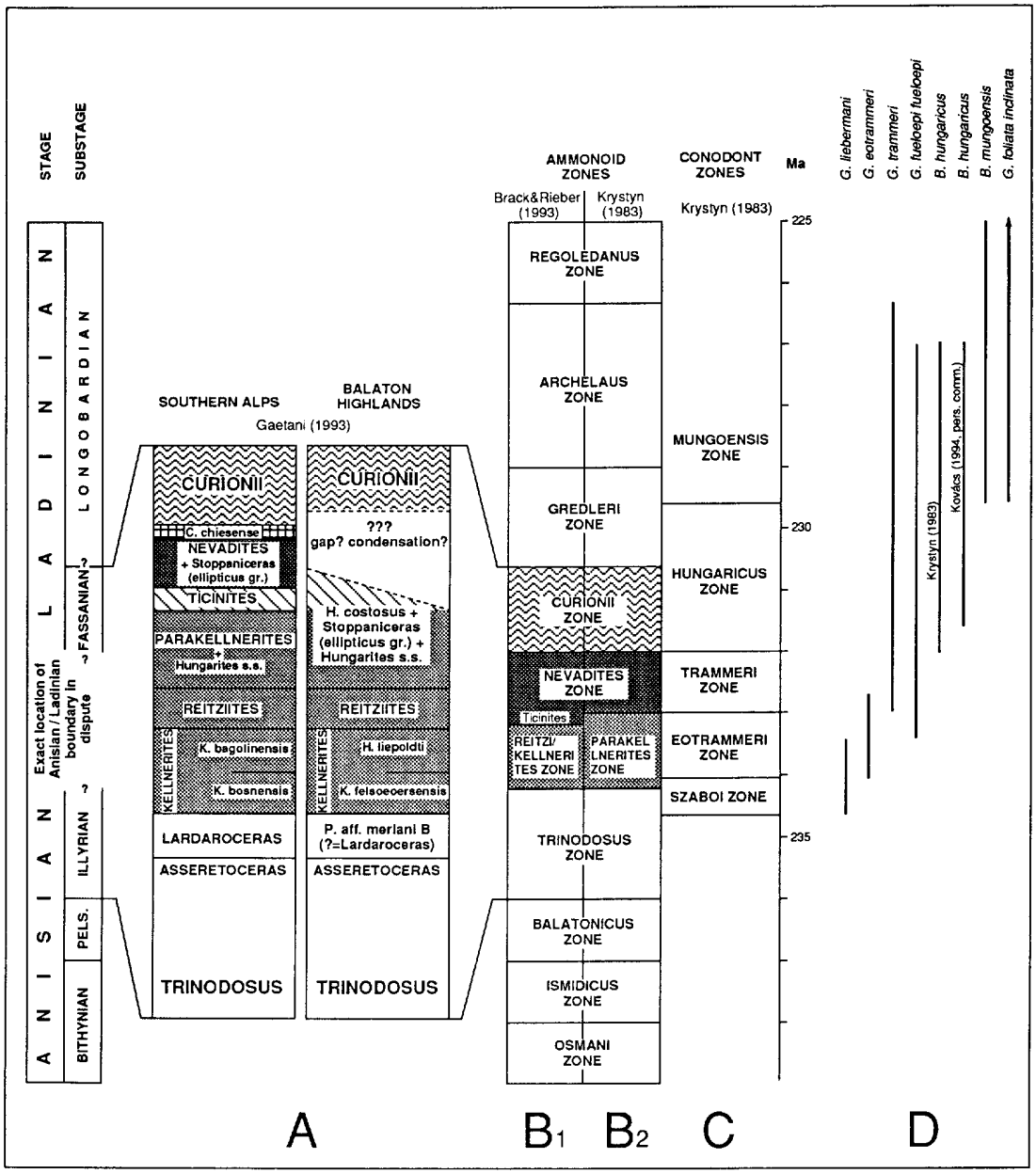

Fig. 4. Southern Alps and Balaton Highlands ammonoid zones across the Anisian/Ladinian boundary (Gaetani, 1993) (A) and Western Tethyan ammonoid zones for the Anisian–Ladinian of Brack and Rieber (1993) (B1) and Krystyn (1983) (B2), correlated with conodont zonation of Krystyn (1983) (C) and with stratigraphic range of the conodont species discussed in the text according to Krystyn (1983) and Kovács (1994) (D). The numerical time-scale is from Brack and Rieber (1993). The exact position of the Anisian/Ladinian boundary remains in dispute (Gaetani, 1993).

occurs from the *H. costosus* horizon (upper Reitzi/Kellnerites Zone) to the upper part of the Archelaus Zone (Kovács et al., 1989; Kovács, 1994). *B. hungaricus* first occurs in the Curionii Zone (Late Fassanian) and ranges up to the upper part of the Archelaus Zone (late Middle Longobardian, Krystyn, 1983). *B. mungoensis* is present from the upper Gredleri to the upper part of the Regoledanus Zones, covering the Middle to Late Longobardian time interval. *G. foliata inclinata* ranges from the upper Gredleri Zone to the upper Austriacum Zone (base of Longobardian to the Late Julian; Kovács and Kozur, 1980; Kovács, 1983; Krystyn, 1983).

The conodont fauna of sample LD30 points to an Illyrian age (i.e., the Trinodosus-Reitzi/Kellnerites interval), whereas the occurrence of the conodont associations of samples ATC1 to ATC5 indicates that the whole of the Fassanian and at least the Middle Longobardian are represented in the upper part of the Han-Bulog Lst. in the Aghia Triada section (Plate I).

Apart from the conodont species, the micropaleontological assemblage and, in particular, the sphinctozoa of the upper lithofacies are characteristic of the Ladinian–Carnian of the Tethys (Senowbari-Daryan, 1990; Mastandrea and Rettori, 1989; Dieci et al., 1968; Flügel et al., 1978; Fois and Gaetani, 1981; Ott, 1967) confirming the presence of post-Anisian sediments.

5. Paleomagnetic analysis

Samples were collected using a portable gasoline-powered drill and oriented by magnetic compass. From each 2.54 cm diameter core sample, two or three standard 11.4 cm^3 specimens were cut. One specimen for each sample was devoted to the study of microfacies, while the remaining specimens were used for paleomagnetic and rock magnetic analyses. The specimens were subjected to stepwise thermal demagnetization. Magnetic remanence measurements were made with a "2G" cryogenic magnetometer housed in a magnetically shielded room with an internal ambient field of about 200 nT. Mineral alteration during heating was monitored with a Bartington Susceptibility Meter (MS2). Magnetization components for individual specimens were picked by eye from orthogonal projections of thermal demagnetization data (Zijderveld, 1967). The standard least squares method (Kirschvink, 1980) was applied to determine the component directions. Section mean directions were determined using standard Fisher statistics (Fisher, 1953).

Orthogonal projections of thermal demagnetization data indicate the presence of three magnetization components at the Aghia Triada section (Fig. 5). A low unblocking temperature "A" component, was eliminated at temperatures below 150°C. The direction of this component (dec. 358.0°, inc. 57.4°, a95 = 2.6°, k = 64) coincides closely with the local present-day field. A "B" component directed southwest and up in geographic coordinates or southwest and down after correction for tilting, was isolated in the 150–420°C temperature range (Fig. 6, Table 1). A third "characteristic" high unblocking temperature "C" component was isolated in the 420–570°C or 670°C temperature range (Fig. 5). At Aghia Triada, this component has dual polarity and is directed southeast and up (northwest and down) in geographic coordinates, or southeast and down (northwest and up) after correction for tilting (Fig. 6, Table 1). Similar directions have been found at Aghia Marina (Table 1).

Natural remanent magnetization intensity values of the samples used for statistical analysis range from about 0.1 to 2 mA/m. Maximum unblocking temperatures are consistent with the presence of magnetite (Figs. 5a, c) and hematite (Fig. 5b). Thermal decay of three axes isothermal remanent magnetization (IRM), obtained with a magnetizing field of 1.3T along the z axis, 0.4T along x, and 0.12T along the y axis (Fig. 7) also shows the presence of two magnetic phases with maximum unblocking temperature of 570°C and 670°C. The three-axes IRM curves give an indication of the coercivity spectra. The phase with maximum unblocking temperature of 570°C is strongly affected by the 0.12T field (Fig. 7b–e), while the phase with maximum unblocking temperature of 670°C is only affected by the 0.4T and 1.3T fields (Fig. 7a, f). These observations lead to the conclusion that the higher coercivity/higher unblocking

PLATE I

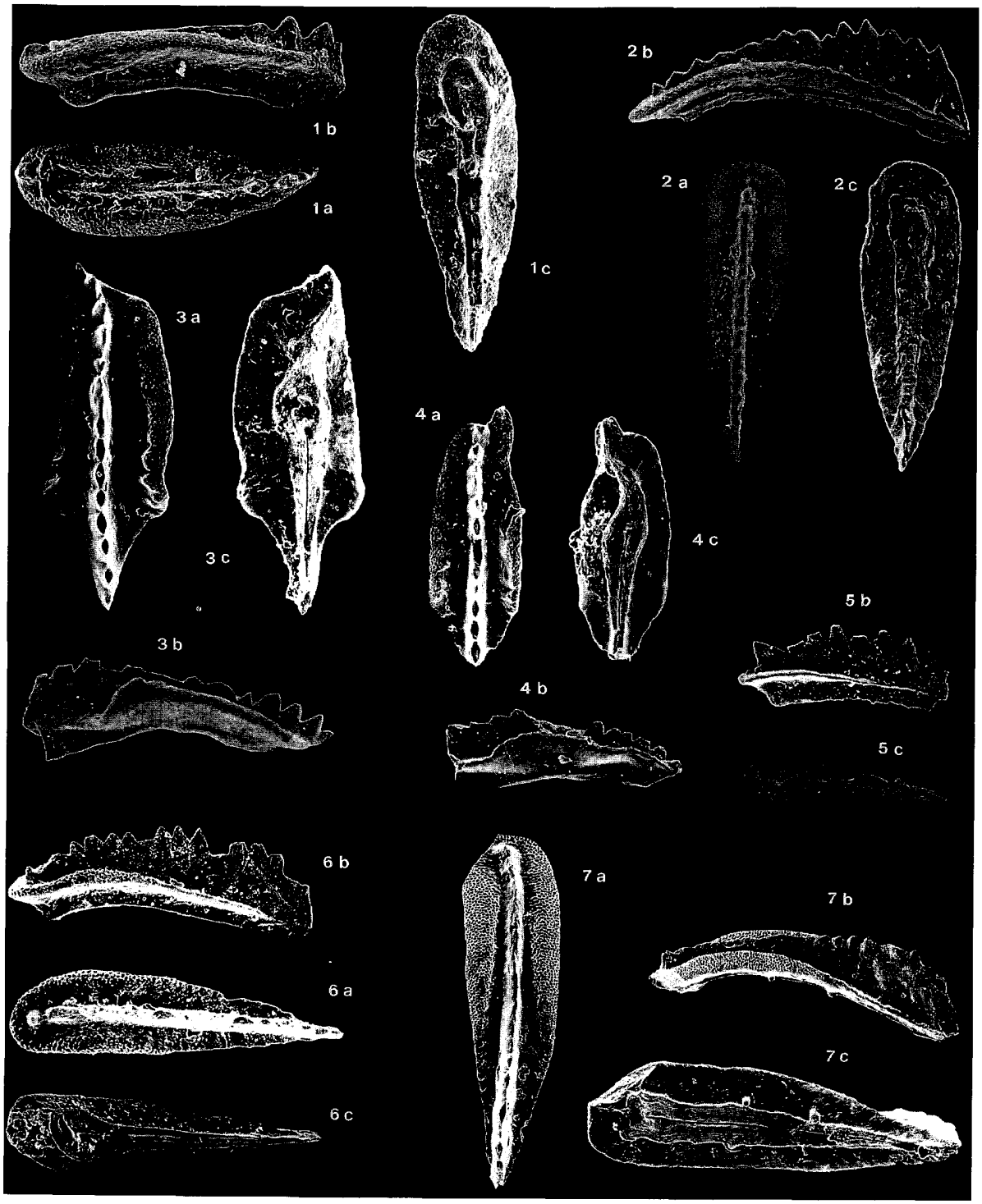

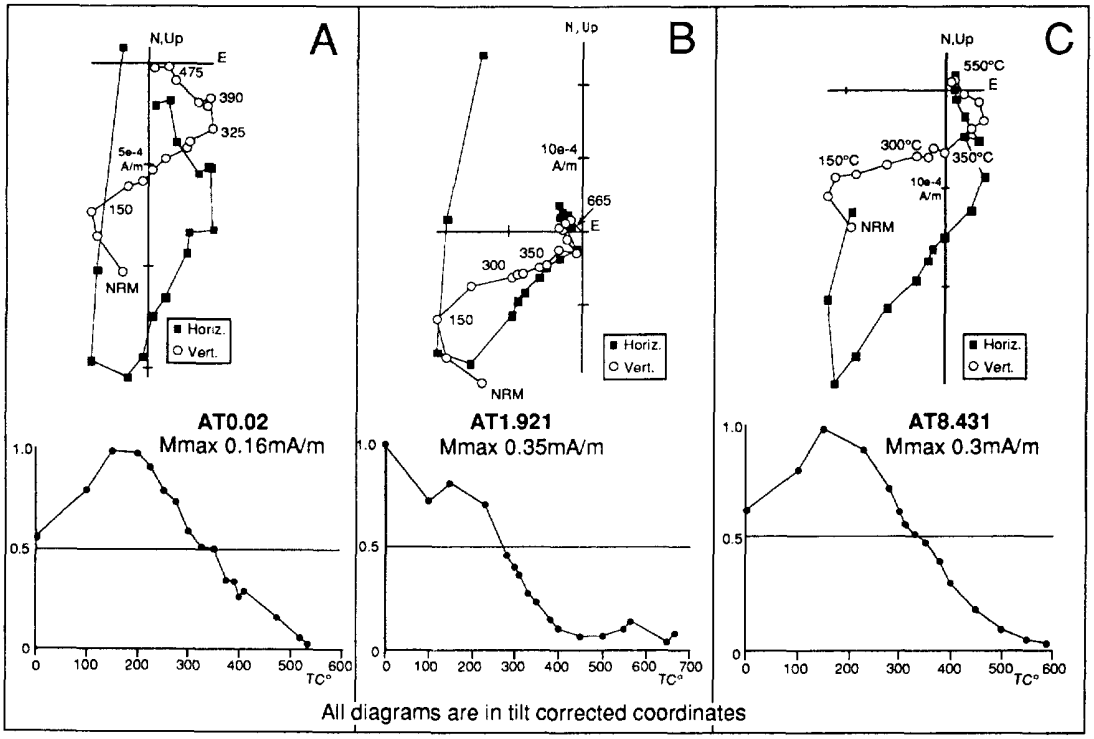

Fig. 5. Orthogonal projections of typical thermal demagnetization behaviour observed at Aghia Triada. The present-day field direction is eliminated in the first few steps. A southwest and up (in situ)/southwest and down (tilt corrected) component is isolated from about 200°C to 400°C. Finally, a dual polarity characteristic component shows up between 400° and 570° or 670°C. Closed symbols are projections onto the horizontal plane and open symbols are projections onto the vertical plane cutting directly through the NRM vector. All diagrams are in tilt corrected coordinates.

temperature phase is hematite, and the lower coercivity/lower unblocking temperature phase is magnetite. In general, samples with the hematite characteristics have a reddish colour, and samples with magnetite characteristics are grey.

The hysteresis parameters for samples from the Aghia Triada section are a function of the proportion of magnetite to hematite in the samples. High values for coercivity (Hc) and coercivity of remanence (Hcr) are characteristic of reddish samples with appreciable hematite content (Fig. 8a, b). The high values of Hcr/Hc and the "wasp-waisted" shape of the hysteresis loops (Figs. 7a, b) imply mixing of a high coercivity hematite and lower

PLATE I

1a–c. *Gondolella trammeri* Kozur. Sample ATC1; a, ×90; b, ×100; c, ×100.
2a–c. *Gondolella liebermani* Kovács and Krystyn. Sample LD30; a, ×75; b, ×75; c, ×75.
3a–c. *Budurovignathus mungoensis* (Diebel), primitive form. Sample ATC3; a, ×110; b, ×100; c, ×110.
4b, c. *Gondolella eotrammeri* Krystyn, juvenile ontogenetic stage. Sample LD30; b, ×100; c, ×100.
5a–c. *Gondolella foliata inclinata* Kovács, medium ontogenetic stage. Sample ATC4; a, ×100; b, ×90; c, ×100.
6a–c. *Gondolella foliata inclinata* Kovács, adult ontogenetic stage. Sample ATC4; a, ×55; b, ×50; c, ×60.
7a–c. *Budurovignathus hungaricus* (Kozur and Vegh). Sample ATC3; a, ×100; b, ×90; c, ×90.
All samples from Aghia Triada section, Han-Bulog Limestone; a = upper view, b = lateral view, c = lower view.

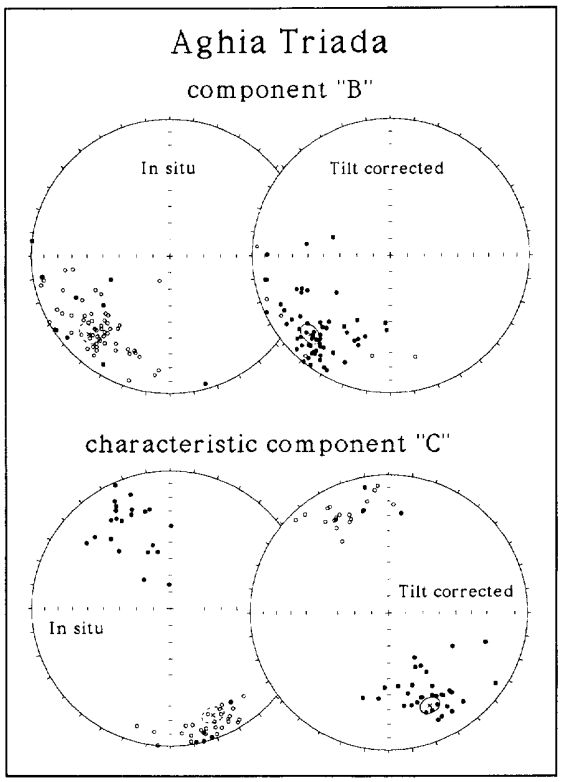

Fig. 6. Equal-area projections showing the "B" component and the characteristic "C" component directions isolated at Aghia Triada, both before and after tilt correction.

coercivity magnetite in these samples. Some samples, particularly grey samples from the upper part of the section, are dominated by magnetite (Fig. 8c). For these samples the values of Mr/Ms (saturation remanence/saturation magnetization) and Hcr/Hc lie in the Pseudo-Single Domain (PSD) field according to the criteria of Day et al. (1977).

6. Discussion

The Aghia Triada section provides the first magnetostratigraphy which can be correlated to the Anisian/Ladinian boundary. Following the polarity zone nomenclature introduced by Alvarez et al. (1977), the Anisian/Ladinian boundary falls into polarity zone "Hydra C+" (Fig. 3). Ammonoid biostratigraphy of the Han-Bulog Lst. of Hydra is due to Renz (1931), subsequent conodont biostratigraphy (Angiolini et al., 1992; this paper) has considerably improved the stratigraphic control in this section. Molina Garza et al. (1991) worked out a Triassic magnetic polarity time scale mainly based on published continental red bed sections from western North America, Canada, Greenland, Spain and China. Although the lack of biostratigraphic control in these sections does not allow precise correlation to stage boundaries

Table 1
Site-mean "B" and characteristic "C" component magnetization directions for Aghia Triada and Aghia Marina sections.

Site	Component designation	*Tb* (°C)	*N*	D_s (°)	L_s (°)	K_s	$(a95)_s$ (°)	D_{tc} (°)	I_{tc} (°)	K_{tc}	$(a95)_{tc}$ (°)	$(Plat)_s$ (°)	$(Plat)_{tc}$ (°)
Ag. Triada	B	150–420	67	225.8	−19.5	10	5.7	225.2	19.6	11	5.6	7N–13N	7N–13N
Ag. Marina	B	200–460	16	210.3	−38	29	6.9	202.1	16.3	22	8	16.5N–26N	4N–13N
Ag. Triada	Characteristic	420–570 420–670	56	158.2	−17.7	13	5.5	156.1	26.9	14	5.2		11N–17N
Ag. Triada	Characteristic normal polarity	420–570 420–670	34	160.2	−7.5	20	5.6	153.8	34.3	18	5.8		
Ag. Triada	Characteristic reversed polarity	420–570 420–670	22	333.5	33	15	8.2	338.3	−15.6	15	8.2		
Ag. Marina	Characteristic	600–670	6	303.5	28.2	15	17.8	307.6	−19.2	15	17.8		0–19N

Tb (°C): unblocking temperature range of the component; *N*: number of specimens used for statistical analysis; D_s, I_s and D_{tc}, I_{tc} (°): declination and inclination in in-situ and tilt-corrected coordinates, respectively; k_s,k_{tc}: precision parameter in in-situ and tilt-corrected coordinates, respectively; $(a95)_s$, $(a95)_{tc}$ (°): half-angle of cone of 95% confidence about the mean direction in in-situ and tilt-corrected coordinates, respectively; $(plat.)_s$, $(plat.)_{tc}$ (°): Paleolatitude calculated from in-situ and tilt-corrected directions, respectively.

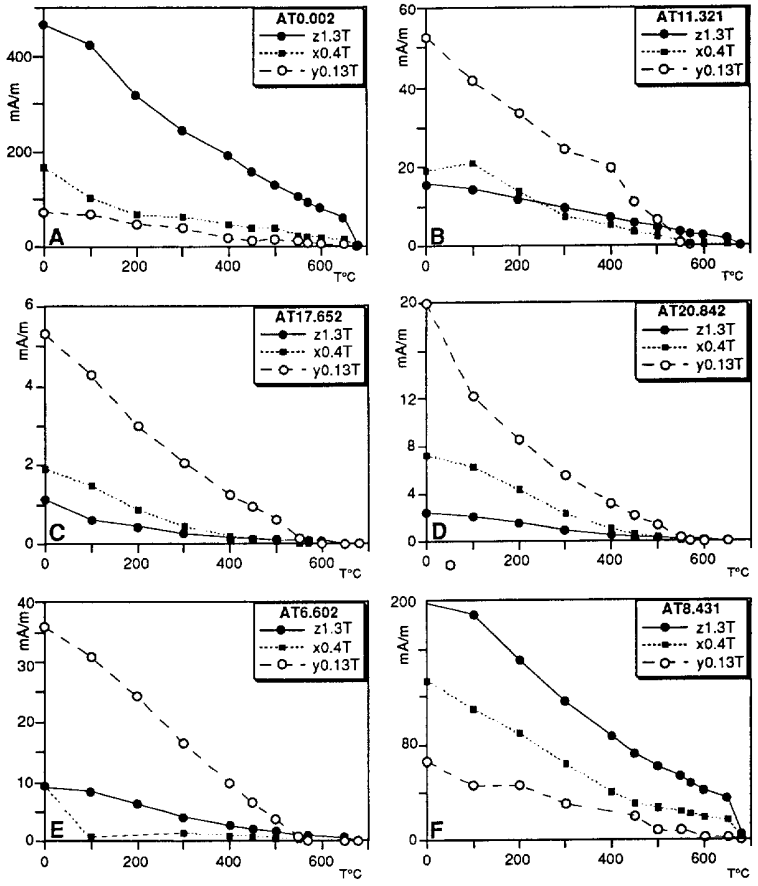

Fig. 7. Thermal decay of three axes Isothermal Remanent Magnetization (IRM) for six Aghia Triada samples, obtained by applying a 1.3T field along the z axis, 0.4T along x, and 0.12T along y. Magnetite, with a low coercivity/570°C maximum unblocking temperature (samples AT17.652, AT20.842, AT6.602) is generally more abundant in the upper portion of the section. Hematite, with a high coercivity/680°C maximum unblocking temperature (samples AT0.002, AT8.431), is typical of the middle-lower portion.

or to conodont-bearing Tethyan sections (and hence to the Hydra sections), the result from the Aghia Triada section can be correlated to the composite Middle Triassic scale of Molina Garza et al. (1991).

Due to the homogeneous attitude of the Han-Bulog Lst. on Hydra (i.e., Aghia Triada N9°E/54°; Aghia Marina N345°E/66°), no fold test is available to constrain the age of the characteristic magnetization. The reversal-bearing characteristic "C" component has a Fisherian distribution, but the positive and negative directions are not perfectly antipodal (Fig. 6; Table 1), probably due to imperfect cleaning of the characteristic "C" component. Assuming this component is Triassic in age and that the sampling sites were located north of the equator at this time (as the generally accepted Middle Triassic paleogeography of the Tethys would imply, Marcoux et al., 1993), the data suggest large scale tectonic rotation since the acquisition of the characteristic remanence.

In Fig. 9, the paleolatitude (determined from the mean inclination) and mean declination for Aghia Triada are plotted with the expected values if this locality had remained part of Europe or NW Africa. The paleolatitude calculated from Aghia Triada characteristic component is in agreement both with the values expected from NW Africa

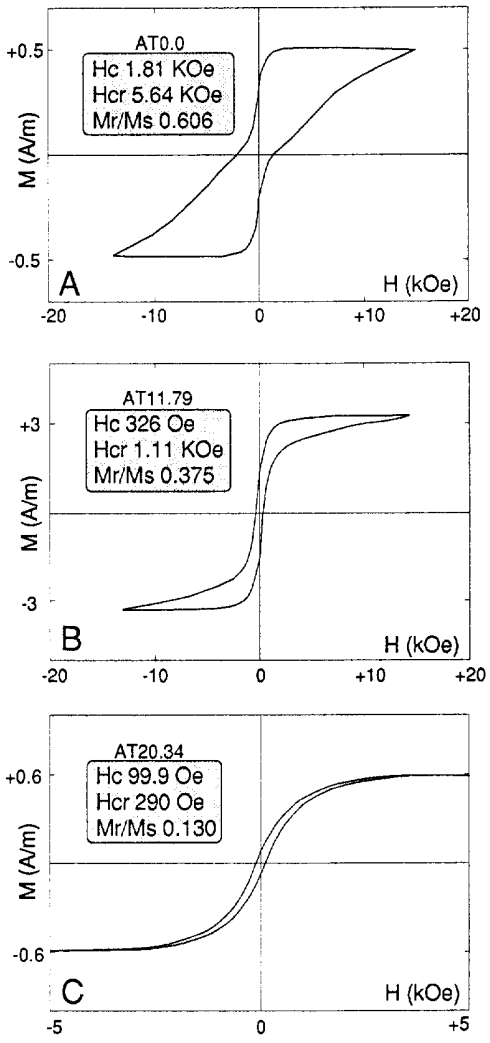

Fig. 8. Hysteresis loops for three Aghia Triada samples. The high values of coercivity of remanence (Hcr)/coercivity (Hc) and the "wasp waisted" shape of the loops (samples AT0.002, AT11.79) implies mixing of a high coercivity hematite and a lower coercivity magnetite in these samples. On the other hand, some samples are dominated by magnetite (AT20.34).

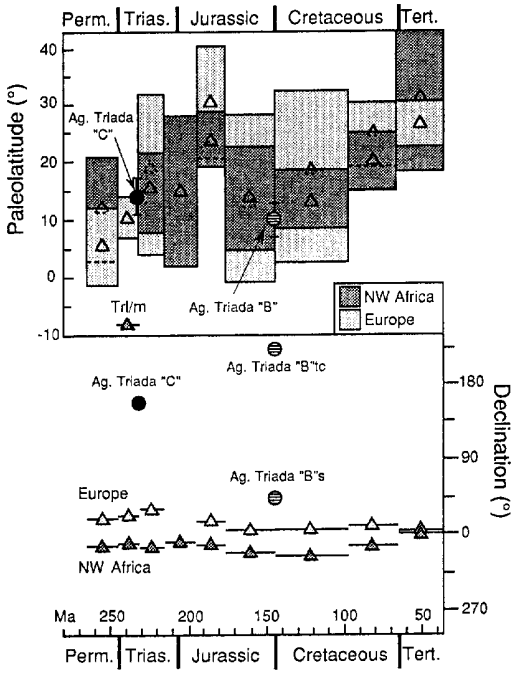

Fig. 9. Values of paleolatitude and declination calculated from the characteristic "C" component (black circles) and "B" component (striped circles) from Aghia Triada, with expected values calculated from Late Permian–Early Tertiary mean paleopoles of Europe ($Q \geq 3$, Van der Voo, 1993) and West Gondwana in the coordinate system of NW Africa (Van der Voo, 1993). The paleolatitude from the characteristic "C" component is in agreement with the Middle Triassic values expected from NW Africa or Europe. The paleolatitude from the "B" component is consistent with a Late Jurassic–Early Cretaceous age for this component. A large declination offset is observed for the mean value of declination of the "C" and "B" components, relative to the European and NW African data. Ag. Triada "B"s and Ag. Triada "B"tc are the mean values of declination of the "B" component in geographic and tilt corrected coordinates, respectively.

paleopoles and with the values expected from European data. On the other hand, comparing the values of declination, the presence of a strong declination offset is apparent (Fig. 9). The Subpelagonian zone, to which Hydra belongs, is generally considered to have developed on the southern margin of the Mesozoic Tethys ocean, and hence to have "African" affinity (Channell and Horváth, 1976; Dixon and Robertson, 1984; Mountrakis et al., 1987). If so, this implies large scale rotation of the sampled thrust sheets on Hydra.

Turnell (1988) and Pucher et al. (1974) published paleomagnetic data from Jurassic rocks outcropping on the Argolis peninsula, a few kilometers NW of Hydra. Turnell (1988) sampled Ammonitico Rosso Lst. of Toarcian to Middle Jurassic age and resolved a magnetization compo-

nent oriented south-west and up in geographic coordinates, which was considered to be a primary Jurassic component. This component has very similar direction to the "B" component observed at Aghia Triada and Aghia Marina. Orthogonal projections of demagnetization data shown by Turnell (1988) indicate that the component content of the remanence has not been fully resolved. The magnetization directions resolved by Turnell (1988) are very similar to the Aghia Triada "B" component. It is unclear whether the "B" component and the component resolved by Turnell (1988) were acquired before or after tilting during a reversed or normal polarity interval, respectively. However, in both cases the value of paleolatitude calculated from the "B" component lies close to the paleolatitude expected from the Late Jurassic–Early Cretaceous mean paleopoles of NW Africa (Fig. 9), and therefore we tentatively infer that the "B" component was acquired as a consequence of nappe emplacement during Late Jurassic time. The declination offset relative to Late Jurassic–Early Cretaceous paleopoles of NW Africa (Fig. 9) implies large scale rotation since acquisition of the "B" component.

If it is accepted that the "characteristic" magnetization component ("C" component) on Hydra is primary and that Hydra was north of the equator in Middle Triassic time, we can infer large scale rotation relative to NW Africa since Middle Triassic time of the sampled thrust sheets on Hydra (Fig. 9), part of this rotation may have occurred prior to Late Jurassic acquisition of the "B" component, perhaps in the early stages of Late Jurassic nappe emplacement. Because of the many uncertainties involved, regarding the deformation history of Hydra and the time of acquisition of the "B" component, any model attempting to explain the large scale rotations observed is, at present, purely speculative.

Acknowledgements

G. Muttoni is indebted to Prof. M. Gaetani for useful discussions and suggestions. The authors are grateful to James Ogg, Neil Opdyke, Sándor Kovács and an anonymous reviewer for careful reviews of the manuscript. Paleomagnetic samples have been measured at the paleomagnetics laboratory of the University of Florida and of Lamont-Doherty Earth Observatory. Financial support by Centro CNR Geodinarnica Alpina e Quaternaria, Milano.

References

Alvarez, W., Arthur, M.A., Fisher, A.G., Lowrie, W., Napoleone, G., Premoli-Silva, I. and Roggenthen, W.M., 1977. Upper Cretaceous–Paleocene magnetic stratigraphy at Gubbio, Italy. V. Type section for the Late Cretaceous–Paleocene geomagnetic reversal time scale. Geol. Soc. Am. Bull., 88: 383–389.

Angiolini, L., Dragonetti, L., Muttoni, G. and Nicora, A., 1992. Triassic stratigraphy in the island of Hydra (Greece). Riv. Ital. Paleontol. Stratigr., 98 (2): 137–180.

Baud, A., Jenny, C., Papanikolaou, D., Sideris, C. and Stampfli, G., 1991. New observations on Permian stratigraphy in Greece and geodynamic interpretation. Bull. Geol. Soc. Greece, 25 (1): 187–206.

Baumgartner, P.O., 1985. Jurassic sedimentary evolution and nappe emplacement in the Argolis Peninsula (Peloponnesus, Greece). Mém. Soc. Helv., Sci. Nat., 99, 111 pp.

Brack, P. and Rieber, H., 1993. Towards a better definition of the Anisian/Ladinian boundary: New biostratigraphic data and correlations of boundary sections from the Southern Alps. Eclogae Geol. Helv., 86 (2): 415–527.

Budurov, K., 1975. Die triassischen conodontenprovinze auf dem Territorium Bulgariens. C. R. Acad. Bulg. Sci., 28: 1681–1684.

Channell, J.E.T. and Horváth, F., 1976. The African/Adriatic promontory as a paleogeographical premise for alpine orogeny and plate movements in the Carpatho-Balkan region. Tectonophysics, 35: 71–101.

Day, R., Fuller, M. and Schmidt, V.A., 1977. Hysteresis properties of titanomagnetites: grain-size and compositional dependence. Phys. Earth Planet. Inter., 13: 260–267.

Dieci, G., Antoniacci, A. and Zardini, R., 1968. Le spugne cassiane (Trias medio-superiore) della regione dolomitica attorno a Cortina d'Ampezzo. Boll. Sci. Geol. Ital., 7(2): 94–155.

Dixon, J.E. and Robertson, A.H.F. (Editors), 1984. The geological evolution of the Eastern Mediterranean. Geol. Soc. Spec. Publ., 17, 824 pp.

Fisher, R.A., 1953. Dispersion on a sphere. Proc. R. Soc. London, Ser. A, 217: 295–305.

Flügel, E., Lein, R. and Senowbari-Daryan, B., 1978. Kalkschwämme, Hydrozoen, Algen und Mikroproblematika aus den Cidaris-Schichten (karn. Ober Trias) der Mürztaler Alpen (Steiermark) und des Gosaukammes (Oberösterreich). Mitt. Ges. Geol. Bergbaustud. Österr., 25: 153–195.

Fois, E. and Gaetani, M., 1981. The recovery of reef-building

communities and the role of Cnidarians in carbonate sequences of the Middle Triassic (Anisian) in the Italian Dolomites. Palaeontol. Am., 54: 191–200.

Gaetani, M., 1993. Anisian/Ladinian boundary field workshop, Southern Alps-Balaton Highlands, 27 June–4July 1993. Albertiana, 12: 5–9.

Kirschvink, J.L., 1980. The least squares line and plane and analysis of paleomagnetic data. Geophys. J. R. Astron. Soc., 45: 699–718.

Kissel, C. and Laj, C., 1988. The Tertiary evolution of the Aegean arc: a paleomagnetic reconstruction. Tectonophysics, 146: 183–201.

Kovács, S., 1983. On the evolution of *excelsa*-stock in the Upper Ladinian-Carnian (Conodonta, genus *Gondolella*, Triassic). In: H. Zapfe (Editor), Das Forschungsproject "Triassic on Tethys Realm" (IGCP Project 4). Schr. Erdwiss. Komm., Österr. Akad. Wiss., 5: 107–120.

Kovács, S., 1994. Conodont of stratigraphical importance from the Anisian/Ladinian boundary interval of the Balaton Highland, Hungary. Riv. Ital. Paleontol. Stratigr., 99 (4): 473–514.

Kovács, S. and Kozur, H., 1980. Stratigraphische Reichweite der wichtigsten Conodonten (ohne Zahnreihenconodonten) der Mittel- und Obertrias. Geol. Paläontol. Mitt. Innsbruck, 10: 47–78.

Kovács, S., Less, G., Piros, O., Réti, Z. and Róth, L., 1989. Triassic formations of the Aggtelek-Rudabánya Mountains (Northeastern Hungary). Acta Geol. Hung., 32 (1–2): 32–62.

Kovács, S., Nicora, A., Szabo, I. and Balini, M., 1990. Conodont biostratigraphy of Anisian/Ladinian boundary sections in the Balaton Upland (Hungary) and in the Southern Alps (Italy). Cour. Forsch. Inst. Senckenberg, 118: 171–195.

Krystyn, L., 1983. Das Epidauros-Profil (Griechenland)—ein Betrag zur Conodonten-Standardzonierung des tethyalen Ladin und Unterkarn. In: H. Zapfe (Editor), Das Forschungsproject "Triassic on Tethys Realm" (IGCP Project 4). Schr. Erdwiss. Komm., Öster. Akad. Wiss., 5: 231–258.

Marcoux, J., Baud, A., Ricou, L.E., Gaetani, M., Krystyn, L., Bellion, Y., Guiraud, R., Moreau, C., Besse, J., Gallet, Y. and Thieveniaut, H., 1993. Late Anisian (237 to 234 Ma). In: J. Dercourt, L.E. Ricou, B. Vrielynck (Editors), Atlas Tethys Palaeoenvironmental Maps. Explanatory Notes. Gauthier-Villars, Paris, pp. 113–134.

Mastandrea, A. and Rettori, R., 1989. Presenza di una associazione a Sphinctozoi (Poriferi) nei corpi carbonatici della Formazione di Monte Facito (Appennino Meridionale). Atti Soc. Nat. Mat. Modena, 120: 15–26.

Molina-Garza, R.S., Geissman, J.W., Van der Voo, R., Lucas, S.G. and Hayden, S.N., 1991. Paleomagnetism of the Moenkopi and Chinle Formations in Central New Mexico: Implications for the North America Apparent Polar Wander Path and Triassic Magnetostratigraphy. J. Geophys. Res., 96: 14,239–14,262.

Mountrakis, D., Patras, D., Kilias, A., Pavlides, S. and Spyropoulos, N., 1987. Structural geology of the Internal Hellenides and their role to the geotectonic evolution of the Eastern Mediterranean. Acta Nat. Ateneo Parmense, 23: 147–162.

Ott, E., 1967. Segmentierte Kalkschwämme (Sphinctozoa) aus der alpinen Mitteltrias und ihre Bedeutung als Riffbildner im Wettersteinkalk. Bayer. Akad. Wiss. Abh., N.F., 131: 1–10.

Pucher, R., Bannert, D. and Fromm, K., 1974. Paleomagnetism in Greece: indications for relative block movement. Tectonophysics, 22: 31–39.

Renz, C., 1906. Trias und Jura in der Argolis. Z. Dtsch. Geol. Ges., 58: 379–395.

Renz, C., 1931. Die Bulogkalke der Insel Hydra (Ostpeloponnes). Eclogae Geol. Helv., 24: 53–60.

Rettori, R., Angiolini, L. and Muttoni, G., 1994. Lower and Middle Triassic foraminifera from the Eros Limestone, Hydra Island, Greece. J. Micropaleontol., in press.

Römermann, H., Graf, W., Huckriede, P., Jacobshagen, V., Kahler, F., Walliser, H., Zapfe, H. and Bornovas, J., 1981. Hydra: In the collection Geologic Maps 1:50,000. Geol. Surv. Greece, I.G.M.E., Athens.

Schäfer, P. and Senowbari-Daryan, B., 1984. The Upper Triassic Pantokrator Limestone of Hydra, Greece: an example of a prograding reef complex. Facies, 6: 147–164.

Senowbari-Daryan, B., 1990. Die Systematishe Stellung der Thalamiden Schwämme und ihre Bedeutung in der Erdgeschichte. Geol. Rundschau, 61: 708–730.

Turnell, H.B., 1988. Mesozoic evolution of Greek microplates from paleomagnetic measurements. Tectonophysics, 155: 307–316.

Van der Voo, R., 1993. Paleomagnetism of the Atlantic, Tethys and Iapetus Oceans. Cambridge Univ. Press, Cambridge, 411 pp.

Wendt, J., 1973. Cephalopod accumulations in the Middle Triassic Hallstatt-Limestone of Jugoslavia and Greece. N. Jahrb. Geol. Paläontol., 28 (4): 624–640.

Zijderveld, J.D.A., 1967. A.C. demagnetization of rocks, analysis of results. In: D.W. Collinson, K.M. Creer and S.K. Runcorn (Editors), Methods in Paleomagnetism. Elsevier, Amsterdam, pp. 254–286.